Macromolecules

pubs.acs.org/Macromolecules Article

Correlation between Locally Ordered (Hydrogen-Bonded) Nanodomains and Puzzling Dynamics of Polymethysiloxane Derivative

Magdalena Tarnacka,* Karolina Jurkiewicz, Barbara Hachuła, Zaneta Wojnarowska, Roman Wrzalik, Rafał Bielas, Agnieszka Talik, Paulina Maksym, Kamil Kaminski,* and Marian Paluch

Cite This: *Macromolecules* 2020, 53, 10225−10233

Read Online

ACCESS | Metrics & More | Article Recommendations | Supporting Information

ABSTRACT: We examined the behavior of poly(mercaptopropyl)methylsiloxane (PMMS), characterized by a polymer chain backbone of alternate silicon and oxygen atoms substituted by a polar pendant group able to form hydrogen bonds (−SH moiety), by means of infrared (FTIR) and dielectric (BDS) spectroscopy, differential scanning calorimetry (DSC), X-ray diffraction (XRD), and rheology. We observed that the examined PMMS forms relatively efficient hydrogen bonds leading to the association of chains in the form of ordered lamellar-like hydrogen-bonded nanodomains. Moreover, the recorded mechanical and dielectric spectra revealed the presence of two relaxation processes. A direct comparison of collected data and relaxation times extracted from two experimental techniques, BDS and rheology, indicates that they monitor different types of the mobility of PMMS macromolecules. Our mechanical measurements revealed the presence of Rouse modes connected to the chain dynamics (slow process) and segmental relaxation (a faster process), whereas in the dielectric loss spectra we observed two relaxation processes related most likely to either the association−dissociation phenomenon within lamellar-like self-assemblies or the sub-Rouse mode (α'-slower process) and segmental (α-faster process) dynamics. Data presented herein allow a better understanding of the peculiar dynamical properties of polysiloxanes and associating polymers having strongly polar pendant moieties.

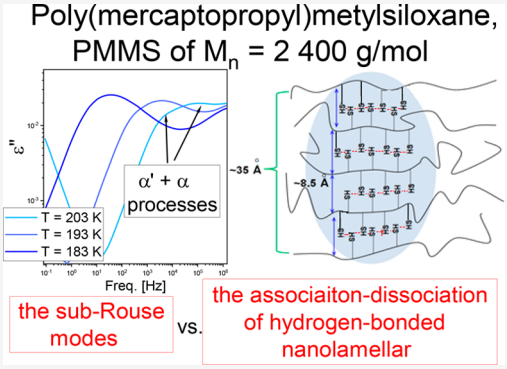

INTRODUCTION

Polysiloxanes (or silicones) are an important class of polymers having backbone consisted of alternate silicon and oxygen atoms.[1] Because of the highly flexible structure, low chemical reactivity and toxicity, and high thermal stability, they are extensively used in, for example, adhesives, households, medicines, lubricants, textiles, and electronics industries, just to name a few.[2−7] Because of this enormous versatility of applications, great effort is put into designing new enhanced siloxane-based materials.[8−13] Nevertheless, it should be pointed out that this progress cannot be achieved without comprehensive studies allowing us to understand behavior and, most importantly, connect the desired properties of produced siloxane-based compounds with their structure. One can recall that the two of the most studied polysiloxanes are poly(dimethylsiloxane) (PDMS, Figure 1a) and poly(methylphenylsiloxane) (PMPS, Figure 1b). Accordingly to the classification based on the geometric dipole arrangements in polymer given by Stockmayer,[14] both of them are considered as type B polymers, where the dipole moment is perpendicularly attached to the main chain backbone.[15,16]

Recent studies of hydroxyl-terminated PDMS (assigned as HO-PDMS-OH) revealed two well-distinguishable loss peaks in the dielectric spectra of this polymer.[17] Interestingly, a similar scenario was also noted in the mechanical data, which allowed the authors to identify the α-process (faster mode) and an additional slower one, which, by the analogy to the monohydroxy alcohols, was assigned to the mobility occurring within hydrogen-bonded supramolecular structures. Additionally, an increased ability to form self-assemblies (due to the presence of hydroxyl terminal groups in HO-PDMS-OH) leads also to a different molecular weight dependence of the glass transition temperature, T_g. In PDMS, T_g increases with molecular weight, M_n, up to some limiting value of T_g[16] according to the Fox−Flory relation.[18,19] In the case of HO-PDMS-OH, an opposite scenario was noted. In these polymers, T_g decreases with M_n. Nevertheless, the glass transition temperature of HO-PDMS-OH reaches a similar

Received: June 1, 2020
Revised: September 11, 2020
Published: November 10, 2020

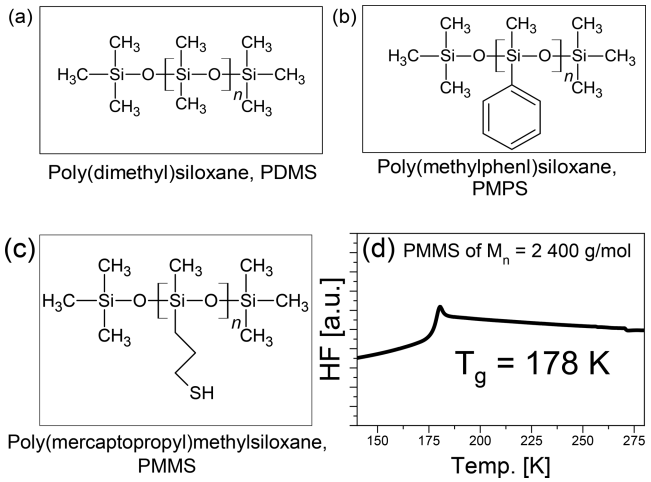

Figure 1. (a) Chemical structures of PDMS (a), PMPS (b), and studied poly(mercaptopropyl)methylsiloxane, labeled as PMMS (c), as well as its DSC thermogram (d).

value as that estimated for PDMS in the high-molecular-weight range.[17]

Further photon correlation spectroscopy (PCS) measurements performed on the low-molecular-weight PMPS also demonstrated the presence of the two processes at first assigned to the local segmental motion (a faster process) and chain diffusion (slower one).[20,21] However, systematic studies indicated that although the faster process is indeed the α-relaxation process, the slower one reflects the so-called sub-Rouse modes of time and length scales intermediate between the Rouse and segmental ones.[22−24] Additional complementary PCS experiments on PMPS and various poly(methyl-*p*-tolylsiloxane)s (PMpTS) confirmed that both processes originate from the molecular motions of comparable units, but of different cooperativity.[25,26] In this context, it is also worthwhile to remind that recent studies on various PMPS, both bulk and confined into alumina templates, also revealed the presence of sub-Rouse modes on the low-frequency flank of the segmental relaxation process in dielectric loss spectra.[27,28] Note that no data on the presence of sub-Rouse modes within PDMS were reported so far.

Differences in the dynamics and number of relaxation modes detected in PDMS and PMPS were discussed in terms of the larger steric hindrance effect posed by the phenyl pendant unit in the latter system that influenced the intermolecular cooperativity. Hence, it is interesting to ask the following: What is going to happen when the methyl side group of PDMS is replaced by a long pendant moiety able to form the hydrogen bonds? Will the sub-Rouse modes be observed or rather the Debye process? How differently will it behave in comparison to PDMS (including HO-PDMS-OH) and PMPS? To answer all of these questions, we studied the behavior of the PDMS derivative, poly(mercaptopropyl)methylsiloxane (PMMS), where the one methyl group was replaced by an alkyl pendant chain terminated with the thiol/sulfanyl (−SH) moiety (see Figure 1c). One can mention that the ability to form the hydrogen-bonded supramolecular structures is very weak in the case of thiol materials. However, it is true only for systems measured at room temperature, where these specific interactions are of comparable strength to the typical van der Waals forces.[29,30] At lower temperatures, this situation is much different since the thiol moiety is capable of creating stronger H-bonds that affect the structure and properties of the given system. Therefore, we expect that an increasing steric hindrance induced by the presence of an alkyl pendant group terminated by the H-bonding moiety might help us to better understand the puzzling dynamics of siloxane-based materials and properties of associating polymers[31,32]—a new generation of systems intentionally designed to reveal non-covalent interactions, that is, H-bonding, metal−ligand bonding, $\pi-\pi$ interactions, ionic bonding, and host−guest interactions.[33] This targeted modification is aimed to produce novel macromolecules characterized by the structural reversibility leading to the unique and most-needed features, such as recyclability, degradability, stimuli responsivity, self-healing, and shape-memory behavior.[34]

EXPERIMENTAL SECTION

Materials. Poly(mercaptopropyl)methylsiloxane homopolymer (PMMS, 75−150 cSt) was purchased from Gelest and used as received (molecular weight, M_{nSEC} = 2400 g/mol, dispersity, $Đ$ = 1.26, determined by Viscotek TDA 305 triple detection, THF as eluent). The studied PMMS is a water-like thin liquid with the glass transition temperature T_g = 178 K (see Figure 1d). Note that no trace of crystallization was observed on both cooling and heating calorimetric scans.

Differential Scanning Calorimetry (DSC). Calorimetric measurements of PMMS were performed by a Mettler-Toledo DSC apparatus equipped with a liquid nitrogen cooling accessory and an HSS8 ceramic sensor (heat flux sensor with 120 thermocouples). Temperature and enthalpy calibrations were performed by using indium and zinc standards. The sample was prepared in an open aluminum crucible (40 μL) outside the DSC apparatus and measured on heating from 150 to 298 K at a constant heating rate of 10 K/min.

Temperature-Modulated Differential Scanning Calorimetry (TMDSC). Using a stochastic TMDSC technique implemented by a Mettler-Toledo TOPEM , we analyzed the dynamic behavior of PMMS in the frequency range from 4 to 30 mHz in one single measurement at a heating rate of 0.5 K/min. In the experiment, the temperature amplitude of the pulses of 0.5 K was selected with a switching time range with minimum and maximum values of 15 and 30 s, respectively. The calorimetric structural relaxation times, $\tau_{\alpha c} = 1/2\pi f$, were determined from the temperature dependences of the real part of the complex heat capacity, $C_p'(T)$, obtained at different frequencies in the glass transition region for PMMS. The glass transition temperature T_g was determined for each frequency as the temperature of the half-step height of $C_p'(T)$.

Fourier Transform Infrared Spectroscopy (FTIR). FTIR measurements were performed with the use of a Nicolet iS50 FTIR spectrometer (Thermo Scientific) in the frequency range from 800 to 4000 cm^{-1}. The bands below 800 cm^{-1} were not taken into account due to the absorption of CaF_2 windows. FTIR spectra were collected with the spectral resolution of 4 cm^{-1}, taking 32 scans per spectrum. The temperature experiment of FTIR measurements was regulated/controlled through a Linkam THMS 600 heating/cooling stage (Linkam Scientific Instruments Ltd., Surrey, UK) mounted inside the sample stage of the IR spectrometer. The temperature changes were measured with the cooling rate of 10 K min^{-1}, and the temperature stabilization accuracy was equal to 0.1 K.

FTIR spectra of PMMS solutions in carbon tetrachloride (CCl_4) were recorded by using a transmission solution cell with KBr (0.01 M) and NaCl (0.1 M) windows with a path length of 1.03 and 0.26 mm, respectively. For each solution, 16 scans were collected in the range from 400 to 4000 cm^{-1} with a spectral resolution of 4 cm^{-1}.

X-ray Diffraction (XRD). The temperature-dependent wide-angle XRD measurements were performed by using a Rigaku-Denki D/MAX RAPID II-R diffractometer with Ag K_α radiation (wavelength λ = 0.5608 Å), equipped with an incident beam (002) graphite monochromator and an image plate detector in the Debye−Scherrer geometry. The sample was measured in glass capillary with a diameter

https://dx.doi.org/10.1021/acs.macromol.0c01289
Macromolecules 2020, 53, 10225−10233

of 1.5 mm. An empty capillary was measured under the same conditions and used for background subtraction. The temperature was controlled by using an Oxford Cryostream Plus and Compact Cooler in the range from 193 to 293 K. The obtained two-dimensional diffraction patterns were converted into one-dimensional intensity data versus the scattering vector, $Q = 4\pi \sin\theta/\lambda$, where 2θ is the scattering angle.

Broadband Dielectric Spectroscopy (BDS). Dielectric permittivity, $\varepsilon^*(\omega) = \varepsilon'(\omega) - i\varepsilon''(\omega)$, values at ambient pressure were measured by using the impedance analyzer (Novocontrol Alpha) over a frequency range from 1×10^{-1} to 3×10^6 Hz. The samples were placed between two stainless-steel electrodes (diameter: 10 mm; gap: 0.05 mm) and mounted inside a cryostat. During the measurement, each sample was maintained under dry nitrogen gas flow. The temperature was controlled by a Quatro Cryosystem using a nitrogen gas cryostat, with stability better than 0.1 K. The temperature-dependent dielectric measurements were performed in the range from 173 to 303 K. It should be mentioned that for the majority of glass formers dielectric spectra are usually shown in a permittivity, ε^*, representation (see Figure 5). However, to compare results obtained from mechanical and dielectric investigations, usually, latter data are converted to the modulus representation.[35] Electric modulus and complex permittivity are related as follows:

$$M^*(\omega) = \frac{1}{\varepsilon^*(\omega)} = M'(\omega) + iM''(\omega) \tag{1}$$

where real (M') and imaginary (M'') parts of M^* have the following forms:

$$M'(\omega) = \frac{\varepsilon'(\omega)}{(\varepsilon'(\omega))^2 + (\varepsilon''(\omega))^2} \text{ and } M''(\omega) = \frac{\varepsilon''(\omega)}{(\varepsilon'(\omega))^2 + (\varepsilon''(\omega))^2} \tag{2}$$

By use of eq 2, dielectric data were recalculated from $\varepsilon''(\omega)$ to $M''(\omega)$ as shown in Figure S3.

Collected spectra in electric modulus representation were further analyzed by the superposition of two or three Havriliak–Negami (HN) functions:[36]

$$M^*(\varpi) = \mathrm{Im}\sum_{i=1}^{2}\left(M_\infty + \frac{\Delta M_i}{[1 + (-i(\varpi\tau_{\mathrm{HN}-M_i})^{-1})^{\alpha_{\mathrm{HNi}}}]^{\beta_{\mathrm{HNi}}}}\right) \tag{3}$$

where α_{HN} and β_{HN} are the shape parameters representing the symmetric and asymmetric broadening of given relaxation peaks, ΔM is the dielectric relaxation strength, $\tau_{\mathrm{HN}-M}$ is the HN relaxation time in electric modulus representation, and ϖ is an angular frequency ($\varpi = 2\pi f$).

To estimate the value of the glass transition temperature, T_g, the data presented in Figure 6 were fitted by using the Vogel–Fulcher–Tamman (VFT) equation:[37−39]

$$\tau_\alpha = \tau_\infty \exp\left(\frac{D_T T_0}{T - T_0}\right) \tag{4}$$

where τ_∞ is the relaxation time at finite temperature, D_T is the fragility parameter, and T_0 is the temperature, where τ goes to infinity. To calculate the activation barrier for the γ-process, the Arrhenius equation was used:

$$\tau_\alpha = \tau_\infty \exp\left(\frac{\Delta E}{k_B T}\right) \tag{5}$$

where k_B is the Boltzmann constant and ΔE is the activation energy.

Shear Rheology. The viscosity of PMMS was determined by means of an ARES G2 rheometer. The viscosity measurement in the vicinity of the liquid–glass transition was performed by using aluminum parallel plates geometry (diameter = 8 mm). For the oscillation-frequency rheological experiments, the investigated sample was tested in the frequency range from 0.1 to 100 rad s^{-1} (12 points per decade) and over the temperature range T = 177–203 K.

RESULTS AND DISCUSSION

To study the temperature evolution of the hydrogen (H)-bonding pattern in PMMS, the system was characterized by IR spectroscopy. Note that in our study we focused only on PMMS of molecular weight M_n = 2400 g/mol, which is a liquid with T_g = 178 K (Figure 1d). This is important information, considering that only in the case of low-molecular-weight polymers, similarly to HO-PDMS-OH, the formation of the supramolecular structures via H bonds was clearly observed.[17] Just to add that with the elongation of the polymer backbone, the role of specific interactions becomes weaker, and the association process is being suppressed. FTIR measurements were performed from room temperature (T = 293 K) down to the liquid nitrogen temperature (T = 83 K). The evolution of the IR spectra for PMMS as a function of temperature is given in Figure 2. As observed at T = 293 K, PMMS shows the

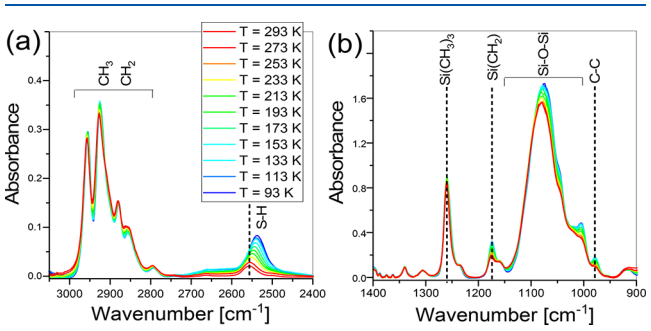

Figure 2. Temperature-dependent evolution of recorded IR spectra (3050–900 cm^{-1}) of PMMS.

intense band located between wavenumber, ν, 3000 and 2800 cm^{-1} (2957, 2927, 2881, 2862, and 2795 cm^{-1}) assigned to the asymmetric and symmetric C–H stretching vibrations of the methyl and methylene groups (ν_{C-H}). The S–H stretching vibration is found as a small peak at 2557 cm^{-1}. According to the literature, the band of free (non-H-bonded) S–H group, ν_{S-H}, is usually located at about 2580–2590 cm^{-1}. Thus, the occurrence of the ν_{S-H} band in the PMMS spectrum at lower wavenumbers can be associated with the hydrogen bond's formation.[40,41] The $Si-CH_3$ groups are easily recognized by a characteristic, very sharp band at 1260 cm^{-1}, whereas the weaker peak appearing at 1175 cm^{-1} is assigned to the deformation vibration of the $Si-CH_2$ groups in the propyl chain (δ_{Si-CH_2}).[42] Both bands confirm that two types of alkyl groups are directly attached to a silicon atom. The origin of the bands at the region of ~900–1000 cm^{-1} can be associated with the C–C stretching vibrations of methylene groups.[42,43] The strongest spectral feature in the IR spectrum of PMMS occurring as a broad band with an absorption maximum at 1080 cm^{-1} arises from the asymmetric Si–O–Si stretching vibrations ($\nu_{as(Si-O-Si)}$).[42,44]

As the temperature gradually decreases to T = 83 K, the intensity of IR bands increases, and they are slightly shifted to lower frequencies. The peaks associated with the C–H groups show the only small red-shift of about 2 cm^{-1} (ν_{C-H}) or 1 cm^{-1} (δ_{Si-CH_2}). Particularly interesting spectral behavior after the temperature drop is observed for the S–H stretching vibration band; that is, the ν_{S-H} band shifts to lower frequencies from 2557 to 2538 cm^{-1} ($\Delta\nu$ = 19 cm^{-1}), and its intensity strongly increases. This red-shift is attributed to the shortening of the S–H bond length and denotes the

https://dx.doi.org/10.1021/acs.macromol.0c01289
Macromolecules 2020, 53, 10225–10233

stronger H-bonding interactions between the S−H groups. The decreasing temperature also leads to a red-shift of the $\nu_{as(Si-O-Si)}$ band; that is, the change of the peak frequency from 1080 to 1074 cm^{-1} is observed ($\Delta\nu$ = 6 cm^{-1}). In this case, the red-shift is associated with deformation of the PMMS structure, involving the elongation of Si−O bonds to accommodate the mercaptopropyl group linked to the inorganic silica chain. This suggests a modification of the polymer backbone conformation as the H-bonding interactions of −SH groups between neighboring chains become stronger with decreasing temperature. Complementary to the temperature-dependent studies, we also decided to perform solution-state FTIR measurement to evaluate the strength of the H bonds and tendency to the association of PMMS (see Figure S1). By use of this method, it was possible to determine the position of the SH stretching vibration peak at 2578 cm^{-1} corresponding to the free (non-hydrogen-bonded) system in very diluted solutions (PMMS concentrations in $CCl_4 \leq 0.01$ M). As PMMS concentration increases (>0.01 M), the ν_{S-H} band is red-shifted, reaching limiting value ~2557 cm^{-1} for neat PMMS. This simple experiment demonstrated that PMMS forms supramolecular structures even at room temperature. Note that also the DLS measurements performed for solutions of PMMS in CCl_4 of various concentrations indicates a formation of small aggregates (see Figure S2).

To obtain further insight into the structure of PMMS during cooling, additional structural (XRD) studies were performed on this polymer at temperature range T = 193−293 K. Interestingly, the diffraction pattern of PMMS at T = 293 K shows two diffuse peaks in the low scattering vector range (see Figure 3a). The more intense reflection at around 1.5 $Å^{-1}$ gives

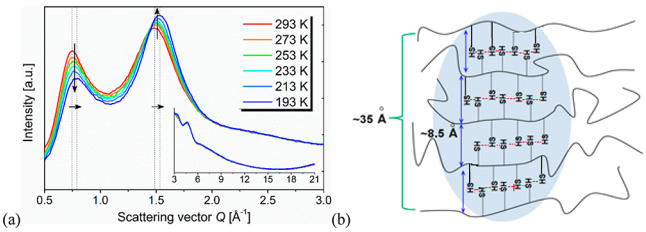

Figure 3. (a) Temperature-dependent evolution of the X-ray diffraction patterns for PMMS, in the low scattering vector range. The inset shows the diffraction patterns in the wide scattering vector range up to 21 $Å^{-1}$. (b) Schematic representation of the internal structure of PMMS via hydrogen bonding (red dashed lines), where a local ordering of chains occurs with more or less parallel alignment of individual chain backbones in lamellar domains.

average periodicity distance $d = 2\pi/Q$ of around 4.2 Å that could be associated with the nearest-neighbor distance of the short-range order between polymer macromolecules within the disordered network. On the other hand, the peak at around 0.75 $Å^{-1}$ arises due to the supramolecular cluster formation and a medium-range order with repeating distance, d, around 8.5 Å. Such a periodicity might correspond to the interchain separation distance when PMMS chain backbones tend to organize closely parallel to each other into lamellar-like domains (see Figure 3b). The determined full width at half-maximum, FWHM, of the prepeak helps to estimate the coherence length, L (the average size of the lamella in the direction perpendicular to PMMS backbone), via the formula $L = 2\pi/\mathrm{FWHM}$. At T = 293 K, the L is equal ~35 Å (3.5 nm).

As temperature decreases down to T = 193 K, a monotonic shift of both diffraction peaks toward higher Q values can be observed, suggesting a grow of polymer density and shortening of interchain distances. Interestingly, the intensity of the main diffraction peak increases, while the width sharpens with a temperature that is a typical behavior due to less thermal motions of the macromolecules, whereas the intensity of the prepeak atypically decreases with lowering the temperature. A similar scenario was observed in H-bonding monohydroxy alcohols[45] and other associating systems.[46] This effect is mostly interpreted as due to a change in the relative orientation of chains or inhomogeneous fluctuation in the density (distribution of chains in the network). In turn, the prepeak width decreases slightly with a temperature drop, and the average size of the ordered regions, L, increases up to 3.7 nm at T = 193 K. This indicates the longer-range ordering of chains due to less thermal motions of molecules and formation of the stronger H bonds via thiol moiety compared to T = 293 K, as found by FTIR investigations. The diffraction pattern in the wide scattering vector range showed in the inset of Figure 3a is mostly related to the intrachain structure of the studied PMMS via hydrogen bonds. As can be seen, this part of the diffraction data do not show any significant changes with decreasing temperature. Although FTIR studies indicated the elongation of Si−O bonds in the PMMS backbone with decreasing temperature, the overall structural motif of PMMS chains is preserved.

To summarize this part, one can state that presence of thiol moieties (having a weak tendency to the formation of the effective H bonds) at the end of alkyl pendant side groups induce association process that gets stronger with lowering temperature. In consequence, this phenomenon leads to the formation of lamellar supramolecular domains consisting of a few chains parallel to each other. What is more, since the examined PMMS has the H-bonding moiety (−SH group, Figure 1c) in every repeatable unit, one can expect that H bonds between neighboring chains will create some kind of cross-links leading to rather ladder-like architecture than the chain or brush-like structure discussed in the case of hydroxyl-terminated HO-PDMS-OH.[17]

In the next step, we performed dielectric measurements in a wide temperature range to characterize the molecular dynamics of PMMS. Unexpectedly, it was found that there is a bimodal loss peak consisted of the two relaxation processes that tend to merge upon approaching the glass transition temperature, T_g (see Figure 4). To visualize this finding in a better way, three representative dielectric loss spectra out of those presented in Figure 4a were separately shown together with the fits composed of single or superposition of the two Havriliak−Negami (HN) functions (see Figures S3 and S4). This kind of data presentation clearly indicated that the latter protocol (two HN functions) yields fits that described the obtained data much better in the whole range of frequencies when compared to the former approach. Note that the fit quality when using only one HN function was markedly worse, especially in the low frequencies (see Figure S4). This implies that the loss peak observed above T_g is, in fact, a bimodal and cannot be considered as broad and asymmetric single relaxation process. Consequently, further, the collected data were analyzed with the use of at least two HN functions (see the Experimental Section). In Figure S5, we plot the HN shape parameters as well as the dielectric strength, $\Delta\varepsilon$, determined for both relaxation processes detected above T_g. As can be seen, α_{HN}

https://dx.doi.org/10.1021/acs.macromol.0c01289
Macromolecules 2020, 53, 10225−10233

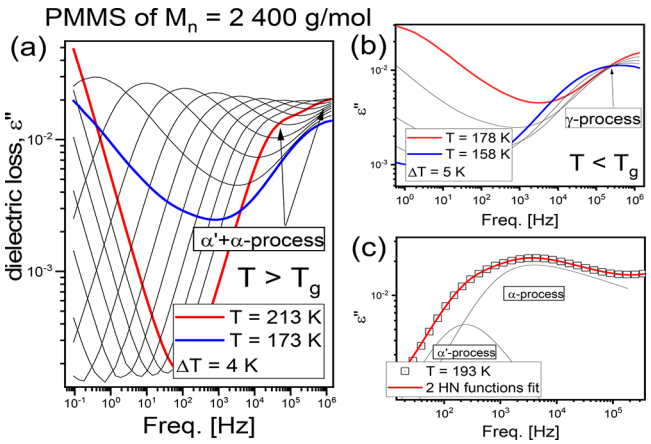

Figure 4. Dielectric loss spectra of the examined PMMS recorded above (a) and below (b) the glass transition temperature. (c) Loss spectrum measured at T = 193 K; the solid red line represents the fit consisted of superposition of the two HN functions (black lines).

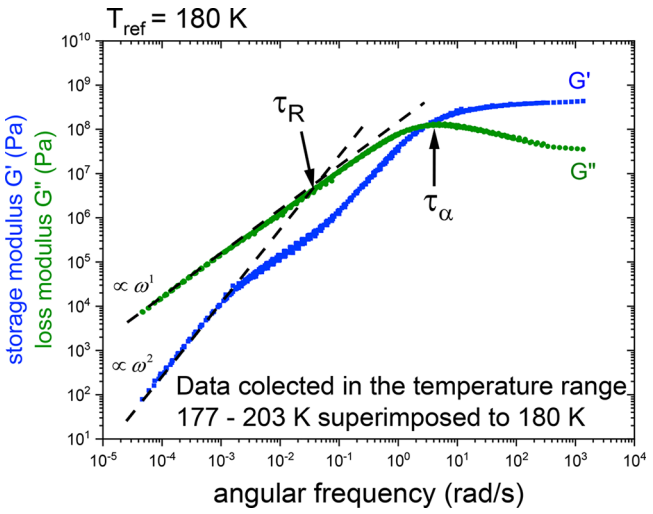

Figure 5. Master curves of measured storage, G', and loss, G'', modulus of examined PMMS collected in the temperature range T = 177−203 K and superimposed at T_{ref} = 180 K.

and β_{HN} of the slow mode (labeled herein as α') are very close to the unity indicating its Debye-like nature. On the other hand, both parameters obtained for the faster (labeled as α) relaxation are much lower than unity, suggesting that it might be the segmental process connected to the viscous flow. One can also mention that $\Delta\varepsilon$ of α' and α remains constant or slightly increases with the lowering temperature, respectively. Nevertheless, it should be mentioned that due to the proximity of both processes, there is quite large uncertainty in the determination of these parameters. Additionally, one can add that with further lowering the temperature below T_g, one secondary relaxation (assigned as γ) appears at high frequencies (see Figure 4b).

One can recall that usually above T_g one prominent α-relaxation process, responsible for the cooperative motions of molecules/segments, can be observed. Although in some specific molecules/polymers, this universal mobility is accompanied by the additional relaxation modes reflecting the motions of larger (sub)units. These extra modes can be considered as related to the mobility within self-assemblies[47,48] (Debye process in low-molecular-weight HO-PDMS-OH[17]), motions of polymer backbone such as chain diffusion (observed in type A polymers[14]), sub-Rouse modes (found in PMPS[27,28]), or local fluctuations of some polar moieties labeled as secondary processes. Nevertheless, taking into account that generally in the case of materials with more than two OH groups per molecule Debye relaxation is barely detectable in dielectric loss spectra,[49,50] it can be supposed that this kind of mobility may not be observed in PMMS that has plenty of SH moieties in one chain (Figure 1c). Moreover, it should be pointed out that the chain dynamics is not dielectrically active for polysiloxanes (considered as type B polymers), which excludes the chain diffusion origin.[17] One can also mention that the sub-Rouse modes are rarely observed by the BDS technique.[51] Hence, taking into account the discussion mentioned above and the puzzling nature of the additional dielectric relaxation process observed above T_g, we have performed comprehensive complementary mechanical measurements.

Master curves of measured storage, G', and loss, G'', modulus of examined PMMS are shown in Figure 5. The presented master curve was constructed from the frequency dependencies of G' and G'' measured within the range of 0.1−100 rad s^{-1} at various temperatures (Figure S7), which were shifted horizontally by the shift factor, α_T, to superimpose at the reference temperature, T_{ref} = 180 K.[52,53] As observed, two prominent processes can be detected, the faster (at higher frequencies) reflecting the segmental motions and an additional one at lower frequencies (Figure 5). Both modes are separated by ∼4 orders of magnitude on the time scale. One can add that a similar situation, with the same difference in relaxation rates, was also reported for various PDMS characterized by different chain ends.[54] In these polymers, the faster and the slower processes were assigned to the segmental motions and Rouse modes (related to the terminal/chain relaxation), respectively. Therefore, by the analogy, this interpretation of G' and G'' spectra of PMMS will be adopted herein. Moreover, a direct comparison of the dielectric and rheological data presented in Figures 4 and 5 revealed that the chain mode does not correspond to any of relaxation processes detected in loss spectra (Figure 4). Moreover, when we compare the loss modulus, G'', spectra with the dielectric modulus, M'', near T_g, one can see that the α-peak recorded in mechanical measurements has much different shape than the one detected in dielectric spectra (see Figure S8). Both findings discussed above indicate that actually both applied techniques monitor a different kind of mobility. Note that to set together the results obtained from the mechanical and dielectric measurements, generally loss G'' and dielectric M'' modulus are compared (see the Experimental Section).

To explore in more detail the molecular dynamics and the origin of the two dielectric relaxation processes detected in the examined PMMS above T_g, we determined and analyzed temperature evolution of their relaxation times, τ (see Figure 6). Note that dielectric τ was estimated from the fitting of collected spectra in the electric modulus representation to the two (or three for the spectra measured close to T_g, where the contribution from the γ-process was significant) HN functions (see Figures S5 and S6). On the other hand, τ_α from the mechanical measurements were calculated by the following equation: $\tau_\alpha = \omega^{-1}$, where ω is a frequency of the $G''(\omega)$ maximum. In the temperature range where the G'' peaks are not visible, the time−temperature superposition (TTS) rule can be applied to determine τ_α. According to this criterion, G'

https://dx.doi.org/10.1021/acs.macromol.0c01289
Macromolecules 2020, 53, 10225−10233

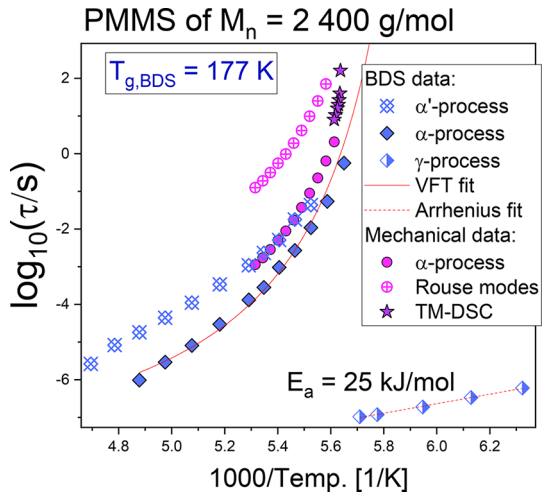

Figure 6. Temperature dependences of relaxation times obtained from dielectric, mechanical, and calorimetric measurements. Red solid and dashed lines represent the best fits to the VFT and Arrhenius equations, respectively (see the Experimental Section).

and G'' spectra collected at various temperature conditions form the master curve when shifted to the reference temperature T_{ref} = 180 K (see Figure 6) and τ_α is taken as the shift factor (α_T). The relaxation time of the slower Rouse modes, τ_R, was estimated by the approach proposed by Patkowski et al.,[26] from the crossover of the two straight lines, representing the dependencies of $\log(G') \sim 2\log(\omega)$ and $\log(G'') \sim \log(\omega)$ in the low frequency. Then, using the relation $\log(\tau(T)) = \log(\tau(T_{ref})) + \log(\alpha_T)$, we obtained their temperature dependencies. The obtained value of τ_α and τ_R were added to Figure 6. Additionally, we also performed temperature-modulated (TM) DSC measurements to determine values of τ_α near T_g (see the Experimental Section), which are also included in Figure 6.

Interestingly, it was found that the relaxation times of the dielectrically active slower process agree well with the $\tau_\alpha(T)$ dependence determined from both TM-DSC and rheological measurements, which might suggest that this process is the segmental (α) relaxation related to the glass transition phenomenon. However, this implies that the faster mode is a secondary relaxation. This interpretation is consistent with the data reported for different kinds of polymers, including polymethacrylates. However, as one can recall generally, the α and secondary β processes merge at high temperatures and tend to separate upon approaching T_g.[55] Moreover, it should be highlighted that the secondary processes are characterized by the Arrhenius-like temperature dependences of relaxation times.[55] These features indicated that the faster process could not be a secondary process. Considering this discussion and the shape parameters determined for both modes, we propose to assign the faster process as the real segmental (α) relaxation related to the glass transition phenomenon and the slower dielectric process (labeled as α') to be connected to sub-Rouse mobility of larger than segmental (sub)units or the association−dissociation process of the formed supramolecular lamellar-like structures as revealed by XRD and FTIR investigations. Note that the terminal relaxation observed in the mechanical measurements and dielectric α' process are found to differ by 2−3 orders of magnitude in time, which exclude the chain diffusion origin of this process (see Figure 6).

For a deeper understanding of this problem, we compared temperature dependencies of the relaxation times obtained for PMMS with two different PDMS able to form H bonds (hydroxyl-terminated HO-PDMS-OH) and the van der Waals polymer (silanol-terminated PDMS). In the case of oligomeric HO-PDMS-OH (M_n < 1100 g/mol), the dielectric loss spectra are dominated by the slower (Debye) relaxation connected to the motions within supramolecular self-assemblies or association phenomena. However, the contribution of this process to the loss spectra decreases with M_n and completely vanishes for polymers with M_n > 2000 g/mol. Note that data for HO-PDMS-OH were taken from ref 17. It should also be noted that both processes observed for HO-PDMS-OH merge when approaching T_g, similarly as in the case of studied PMMS (see Figure S9a). Moreover, the time scale separations between α' (or Debye) and α in both polymers are similar. These similarities might indicate that the slow mode in the dielectric loss spectra of PMMS could be related to the mobility within hydrogen-bonded supramolecular structures. In this context, it is worthwhile to remind that HN parameters describing the shape of the α' mode are very close to one that is characteristic for a Debye process ($\alpha \sim 0.9$ and $\beta \sim 0.8$). Nevertheless, one can emphasize that the Debye-like process observed in PMMS has a significantly lower amplitude than that detected in HO-PDMS-OH. This finding might be connected to different geometry and a large number of −SH moieties capable of forming H bonds that hold local molecular ordering via these specific interactions. PMMS is also characterized by much higher molecular weight (M_n = 2400 g/mol) than the mentioned HO-PDMS-OH (M_n < 1100 g/mol), which also influences differences between both materials. Assuming that indeed the α' relaxation is related to the association process leading to the formation of hydrogen-bonded (ladder-like) structure, we calculated the activation energy of associations, E_{assoc}, from dielectric data. For details, see refs 56 and 57. The estimated value of E_{assoc} is equal to E_{assoc} = 18 kJ/mol. Interestingly, this energy is comparable to the net interaction energy $E \sim 10-16$ kJ/mol determined for mercaptobenzoic acids having a thiol moiety.[58] The discussion mentioned above suggests that the recorded additional dielectric relaxation is a Debye process reflecting the formation of H bonds and supramolecular structure in PMMS as indicated by complementary FTIR and XRD investigations. Briefly, one can to stress that generally for strongly associating systems, apart from the α-process responsible for the vitrification phenomenon, an additional slower mode of still unknown origin (generally of exponential shape) is observed.[59] However, it is not the strict rule since there are many exceptions such as metatoluidine, water, the phenyl derivative of ibuprofen, and so on.[60,61] In our case, this local ordering might indicate the formation of a hydrogen-bonded (ladder-like) structure of the length scale higher than segments. Considering the geometry of the nanoaggreagates presented in Figure 3b, one can postulate that net dipole moment in such situation cancels out. However, it should be mentioned that the ongoing association−dissociation at $\tau_{\alpha'}$ leads to the change in dipole moments resulting in the rise to the α'-process.[56,62]

Additionally, we examined the dynamics of native PDMS (of M_n = 3700 g/mol). Note that the measurements were performed after careful removal of monomer wastes from the purchased material, which contains a significant amount of impurities. Details concerning the purification procedure and the gel permeation chromatography (GPC) data recorded

https://dx.doi.org/10.1021/acs.macromol.0c01289
Macromolecules 2020, 53, 10225−10233

before and after the performed actions are presented in Figure S9. Surprisingly, the dielectric loss spectra of purified PDMS measured above T_g also revealed the presence of the two relaxation processes (see Figure S10b). One can recall that the recent papers devoted to the dynamics of various PDMS derivatives, including PMPS[27,28] and PMpTS,[63] pointed out the presence of the dielectric relaxation process characterized by intermediate time and length scale between chain (Rouse modes) and segmental relaxations, assigned as sub-Rouse modes. Hence, by the analogy to these papers, the slower relaxation can be assigned as the sub-Rouse process, while the faster process is the segmental one in native PDMS. This agrees when we compare T_g = 147 K (for τ_α = 1 s) determined from the temperature evolution of the relaxation times of the faster process with that estimated from calorimetry (T_g = 148 K). As shown in Figure S10, the time-scale separation between sub-Rouse modes and segmental relaxation in the case of measured PDMS of M_n = 3700 g/mol is quite significant. Moreover, both processes do not merge upon decreasing temperature and have a significantly different amplitude with respect to the ones detected in PMMS (see Figure S10a). Nevertheless, even considering results of mechanical measurements and similarities and differences between dynamical behavior of the relaxation processes in PMMS and hydroxyl-terminated and native PDMS, we are not able to unquestionably state whether α' is connected to the motions of either sub-Rouse modes or the association process leading to the formation of medium-range ordered supramolecular lamella-like hydrogen-bonded nanodomains. On the other hand, the faster mode can be assigned as segmental relaxation in PMMS—especially when we take into account that T_g ($T_{g,BDS}$ = 177 K) determined from the dielectric data using the VFT equation (eq 4) agrees well with the one determined from the calorimetric measurements ($T_{g,DSC}$ = 178 K, Figure 1b) and shape parameters of this mode are much different than unity.

As a final point of our investigations, we have also calculated the activation energy, E_a, of the γ-process in the glassy state. For that purpose, we fitted τ_γ presented in Figure 6 to the Arrhenius equation (eq 5). The calculated activation energy reaches E_a = 25 kJ/mol. Such a low value of E_a indicates that the reorientational motions of the alkyl side group terminated with the thiol moiety are responsible for that. However, taking into account that the sum of the activation barrier for the conformation change of the alkyl chain ($E \sim 14$ kJ/mol) and the energy required to break S−H··S bonds ($E_{S-H\cdot\cdot S} \sim 6$ kJ/mol) is comparable to the value of E_a of the γ-process in PMMS, one can assume that this secondary relaxation process is in some way indirectly connected to the dynamics of the hydrogen bonds.

The data reported herein clearly indicated that one has to be careful in the assignment of the molecular origin of the relaxation processes detected in dielectric data of the polymers tending to form supramolecular domains ordered on the nanoscale. Even a close correspondence between relaxation times obtained for a given relaxation process estimated from different techniques does not necessarily mean that they have the same molecular origin.

CONCLUSION

In this paper, we have discussed the results of complementary structural, mechanical, and dielectric studies performed for poly(mercaptopropyl)methylsiloxane (PMMS) characterized by chain backbone of alternate silicon and oxygen atoms substituted by a polar pendant group terminated with the thiol/sulfanyl (−SH) moiety. Interestingly, the performed FTIR and XRD measurements indicated that the examined PMMS forms weak but relatively efficient directional hydrogen bonds between neighboring chains, in a direction perpendicular to the chain backbone and, in consequence, supramolecular lamellar domains. Surprisingly, the collected dielectric spectra revealed the presence of the two relaxation processes at high temperatures, which merge upon cooling. Considering the outcome of XRD and rheological investigations, it was found that α' (the slower process of Debye-like shape) and α (the faster one) processes detected in loss spectra are connected with the association−dissociation process of the locally ordered nanolamellar domains connected via H bonds and segmental motions, respectively. However, it should be mentioned that the collected data do not entirely exclude the sub-Rouse origin of the observed α'-process in PMMS. Data presented herein can be useful to understand the peculiar dynamical properties of associating polymers tending to form mesoscale self-assemblies.

ASSOCIATED CONTENT

Supporting Information

The Supporting Information is available free of charge at https://pubs.acs.org/doi/10.1021/acs.macromol.0c01289.

Experimental details and additional figures including correlation functions, FTIR spectra, the real part of complex permittivity, the fit of dielectric spectra with the one or two HN functions together with the determined relaxation times, frequency dependencies of G' and G'', comparison of normalized shear and dielectric α-peaks, dielectric loss spectra recorded for PMDS of $M_n \sim 4000$ g/mol, temperature dependences of τ determined for PDMS, PMMS, and HO-PMDSM-OH (PDF)

AUTHOR INFORMATION

Corresponding Authors

Magdalena Tarnacka − *Institute of Physics and Silesian Center of Education and Interdisciplinary Research, University of Silesia in Katowice, 41-500 Chorzow, Poland;* orcid.org/0000-0002-9444-3114; Email: magdalena.tarnacka@smcebi.edu.pl

Kamil Kaminski − *Institute of Physics and Silesian Center of Education and Interdisciplinary Research, University of Silesia in Katowice, 41-500 Chorzow, Poland;* orcid.org/0000-0002-5871-0203; Email: kamil.kaminski@us.edu.pl, kamil.kamimski@smcebi.edu.pl

Authors

Karolina Jurkiewicz − *Institute of Physics and Silesian Center of Education and Interdisciplinary Research, University of Silesia in Katowice, 41-500 Chorzow, Poland;* orcid.org/0000-0002-4289-7827

Barbara Hachuła − *Institute of Chemistry, University of Silesia in Katowice, 40-007 Katowice, Poland*

Zaneta Wojnarowska − *Institute of Physics and Silesian Center of Education and Interdisciplinary Research, University of Silesia in Katowice, 41-500 Chorzow, Poland;* orcid.org/0000-0002-7790-2999

https://dx.doi.org/10.1021/acs.macromol.0c01289
Macromolecules 2020, 53, 10225−10233

Roman Wrzalik − *Institute of Physics and Silesian Center of Education and Interdisciplinary Research, University of Silesia in Katowice, 41-500 Chorzow, Poland*

Rafał Bielas − *Institute of Physics and Silesian Center of Education and Interdisciplinary Research, University of Silesia in Katowice, 41-500 Chorzow, Poland;* orcid.org/0000-0002-5129-063X

Agnieszka Talik − *Institute of Physics and Silesian Center of Education and Interdisciplinary Research, University of Silesia in Katowice, 41-500 Chorzow, Poland;* orcid.org/0000-0001-7940-6967

Paulina Maksym − *Institute of Physics and Silesian Center of Education and Interdisciplinary Research, University of Silesia in Katowice, 41-500 Chorzow, Poland;* orcid.org/0000-0002-8506-7102

Marian Paluch − *Institute of Physics and Silesian Center of Education and Interdisciplinary Research, University of Silesia in Katowice, 41-500 Chorzow, Poland*

Complete contact information is available at: https://pubs.acs.org/10.1021/acs.macromol.0c01289

Notes

The authors declare no competing financial interest.

■ ACKNOWLEDGMENTS

M.T. and M.P. are thankful for financial support from the Polish National Science Centre within the OPUS project (Dec. No. 2019/33/B/ST3/00500). R.B. and K.K. are thankful for financial support from the Polish National Science Centre within the SONATA Bis project (Dec. No. 2015/18/B/ST4/00500320). K.J. is thankful for financial support from the Polish National Centre for Research and Development within the LIDER project (Dec. No. LIDER/24/0131/L-10/18/NCBR/2019). K.J. is grateful for the financial support from the Foundation for Polish Science within the START program.

■ REFERENCES

(1) Rahimi, A.; Shokrolahi, P. Application of Inorganic Polymeric Materials. I. Polysiloxanes. *Int. J. Inorg. Mater.* **2001**, *3*, 843−847.

(2) Bhowmick, A. K., Stephans, H. L., Eds.; *Handbook of Elastomers*; Marcel Dekker, Inc.: 1998; pp 551−620.

(3) Polmanteer, K. E. Silicone Rubber, its Development and Technological Progress. *Rubber Chem. Technol.* **1988**, *61*, 470−502.

(4) Liu, Z.; Lu, H.; Hao, S.; Wen, X.; Du, Z. Synthesis and Characterization of (3,4-Difuryl-2,5-dimethyl) Phenyl−Polyvinyl Silicon Oils. *J. Appl. Polym. Sci.* **1995**, *55*, 1733−1738.

(5) Abbasi, F.; Mirzadeh, H.; Katbab, A.-A. Modification of Polysiloxane Polymers for Biomedical Applications: a Review. *Polym. Int.* **2001**, *50*, 1279−1287.

(6) Aliyar, H.; Schalau, G. Recent Developments in Silicones for Topical and Transdermal Drug Delivery. *Ther. Delivery* **2015**, *6*, 827−839.

(7) Colas, A.; Rafidison, P. Silicones in New Pharmaceutical Developments from Formulations to Manufacturing Processes. *Pharma. Chem.* **2005**, *4*, 46−49.

(8) Bischoff, R.; Cray, S. E. Polysiloxane in Macromolecules Architecture. *Prog. Polym. Sci.* **1999**, *24*, 185−219.

(9) Yi, B.; Liu, P.; Hou, C.; Cao, C.; Zhang, J.; Sun, H.; Yao, X. Dual-Cross-Linked Supramolecular Polysiloxanes for Mechanically Tunable, Damage-Healable and Oil-Repellent Polymeric Coatings. *ACS Appl. Mater. Interfaces* **2019**, *11*, 47382.

(10) Klonos, P. A.; Nosach, L. V.; Voronin, E. F.; Pakhlov, E. M.; Kyritsis, A.; Pissis, P. Glass Transition and Molecular Dynamics in Core-Shell-Type Nanocomposites Based on Fumed Silica and Polysiloxanes: Comparison between Poly(dimethylsiloxane) and Poly(ethylhydrosiloxane). *J. Phys. Chem. C* **2019**, *123*, 28427−28436.

(11) Epure, E.-L.; Vasiliu, T.; Hurduc, N.; Neamtu, A. Molecular Modeling Study Concerning the Self-Assembly Capacity of Some Photosensitive Amphiphilic Polysiloxane. *J. Mol. Liq.* **2020**, *300*, 112298.

(12) Shan, S.; Lei, Y.; Lin, Y.; Zhang, A. Slime-inspired Crosslinked Polysiloxanes Networks Based on Reversible Borate-hydroxyl Complexes. *Polymer* **2020**, *186*, 122026.

(13) Xu, C.-A.; Nan, B.; Lu, M.; Qu, Z.; Tan, Z.; Wu, K.; Shi, J. Effects of Polysiloxanes with Different Molecular Weights on *in vitro* Cytotoxicity and Properties of Polyurethane/Cotton−Cellulose Nanofiber Nanocomposite Films. *Polym. Chem.* **2020**, *11*, 5225−5237.

(14) Stockmayer, W. Dielectric Dispersion in Solutions of Flexible Polymers. *Pure Appl. Chem.* **1967**, *15*, 539.

(15) Kirst, K. U.; Kremer, F.; Pakula, T.; Hollingshurst, J. Molecular Dynamics of Cyclic and Linear Poly(dimethylsiloxanes). *Colloid Polym. Sci.* **1994**, *272*, 1420−1429.

(16) Hintermeyer, J.; Herrmann, A.; Kahlau, R.; Goiceanu, C.; Rossler, E. Molecular Weight Dependence of Glassy Dynamics in Linear Polymers Revisited. *Macromolecules* **2008**, *41*, 9335−9344.

(17) Xing, K.; Chatterjee, S.; Saito, T.; Gainaru, C.; Sokolov, A. P. Impact of Hydrogen Bonding on Dynamics of Hydroxyl-Terminated Polydimethylsiloxane. *Macromolecules* **2016**, *49*, 3138−3147.

(18) Fox, T. G., Jr.; Flory, P. J. Second-order Transition Temperatures and Related Properties of Polystyrene. I. Influence of Molecular Weight. *J. Appl. Phys.* **1950**, *21*, 581−591.

(19) Fox, T. G., Jr.; Flory, P. J. The Glass Temperature and Related Properties of Polystyrene. Influence of Molecular Weight. *J. Polym. Sci.* **1954**, *14*, 315−319.

(20) Fytas, G.; Dorfmuller, T.; Chu, B. Photon Correlation Spectra of Poly (Phenylmethyl Siloxane) under High Pressures. *J. Polym. Sci., Polym. Phys. Ed.* **1984**, *22*, 1471−1481.

(21) Ngai, K. L.; Fytas, G. Interpretation of Differences in Temperature and Pressure Dependences of Density and Concentration Fluctuations in Amorphous Poly(Phenylmethy1 Siloxane). *J. Polym. Sci., Part B: Polym. Phys.* **1986**, *24*, 1683−1694.

(22) Ngai, K. L.; Plazek, D. J.; Rizos, A. K. Viscoelastic Properties of Amorphous Polymers. 5. A Coupling Model Analysis of the Thermorheological Complexity of Polyisobutylene in the Glass−Rubber Softening Dispersion. *J. Polym. Sci., Part B: Polym. Phys.* **1997**, *35*, 599−614.

(23) Ngai, K. L.; Plazek, D. J. Thermo-Rheological, Piezo-Rheological, and TVγ - Rheological Complexities of Viscoelastic Mechanisms in Polymers. *Macromolecules* **2014**, *47*, 8056−8063.

(24) Wang, X.; Nie, Y. J.; Huang, G. S.; Wu, J. R.; Xiang, K. W. Dynamic Crossover of the Sub-Rouse Modes in the Glass−Rubber Transition Region in Poly(n-Alkyl Methacrylates) with Different Side Chain Lengths. *Chem. Phys. Lett.* **2012**, *538*, 82−85.

(25) Kriegs, H.; Gapinski, J.; Meier, G.; Paluch, M.; Pawlus, S.; Patkowski, A. Pressure Effects on the α and α' Relaxations in Polymethylphenylsiloxane. *J. Chem. Phys.* **2006**, *124*, 104901.

(26) Patkowski, A.; Gapinski, J.; Pakula, T.; Meier, G. Physical Nature of Complex Structural Relaxation in Polysiloxane-PMpTS: α and α' Relaxations. *Polymer* **2006**, *47*, 7231−7240.

(27) Adrjanowicz, K.; Winkler, R.; Chat, K.; Duarte, D. M.; Tu, W.; Unni, A. B.; Paluch, M.; Ngai, K. L. Study of Increasing Pressure and Nanopore Confinement Effect on the Segmental, Chain, and Secondary Dynamics of Poly(Methylphenylsiloxane). *Macromolecules* **2019**, *52*, 3763−3774.

(28) Tu, W.; Ngai, K. L.; Paluch, M.; Adrjanowicz, K. Dielectric Study on the Well-Resolved Sub-Rouse and JG β-Relaxations of Poly(methylphenylsiloxane) at Ambient and Elevated Pressures. *Macromolecules* **2020**, *53*, 1706−1715.

(29) Adrjanowicz, K.; Jakobsen, B.; Hecksher, T.; Kaminski, K.; Dulski, M.; Paluch, M.; Niss, K. Communication: Slow Supramolecular Mode in Amine and Thiol Derivatives of 2-ethyl-1-hexanol

Revealed by Combined Dielectric and Shear-mechanical Studies. *J. Chem. Phys.* **2015**, *143*, 181102.
(30) Jurkiewicz, K.; Hachuła, B.; Kamińska, E.; Grzybowska, K.; Pawlus, S.; Wrzalik, R.; Kmainski, K.; Paluch, M. Relationship between Nanoscale Supramolecular Structure, Effectiveness of Hydrogen Bonds, and Appearance of Debye Process. *J. Phys. Chem. C* **2020**, *124*, 2672−2679.
(31) Brunsveld, L.; Folmer, B. J. B.; Meijer, E. W.; Sijbesma, R. P. Supramolecular Polymers. *Chem. Rev.* **2001**, *101*, 4071−4098.
(32) De Greef, T. F. A.; Smulders, M. M.; Wolffs, M.; Schenning, A. P. H. J.; Sijbesma, R. P.; Meijer, E. W. Supramolecular Polymerization. *Chem. Rev.* **2009**, *109*, 5687−5754.
(33) Li, S.-L.; Xiao, T.; Lin, C.; Wang, L. Advanced Supramolecular Polymers Constructed by Orthogonal Self-Assembly. *Chem. Soc. Rev.* **2012**, *41*, 5950−5968.
(34) Yang, L.; Tan, X.; Wang, Z.; Zhang, X. Supramolecular Polymers: Historical Development, Preparation, Characterization, and Functions. *Chem. Rev.* **2015**, *115*, 7196−239.
(35) Kremer, F.; Schonhals, A. *Broadband Dielectric Spectroscopy*; Springer: 2003.
(36) Kremer, F.; Schonhals, A. *Broadband Dielectric Spectroscopy*; Springer: Berlin, 2003.
(37) Vogel, H. Temperatura bhangigkeitgesetz der Viskosität von Flüssigkeiten. *J. Phys. Z.* **1921**, *22*, 645−646.
(38) Fulcher, G. S. Analysis of Recent Measurements of the Viscosity of Glasses. *J. Am. Ceram. Soc.* **1925**, *8*, 339−355.
(39) Tammann, G.; Hesse, W. Die Abhängigkeit der Viscosität von der Temperatur bie unterkühlten Flüssigkeiten. *Z. Anorg. Allg. Chem.* **1926**, *156*, 245−257.
(40) de Alencastro, R. B.; Sandorfy, C. A Low Temperature Infrared Study of Self-association in Thiols. *Can. J. Chem.* **1972**, *50*, 3594−3600.
(41) Nyquist, T. In *Interpreting Infrared, Raman, and Nuclear Magnetic Resonance Spectra*; 2001; Vol. 2, Chapter 4, pp 65−83.
(42) Spcrates, G. *Infrared and Raman Characteristic Group Frequencies: Tables and Charts*, 3rd ed.; Wiley: 2001.
(43) Bistričić, L.; Borjanovic, V.; Mikac, L.; Dananić, V. Vibrational Spectroscopic Study of Poly(dimethylsiloxane)-ZnO Nanocomposites. *Vib. Spectrosc.* **2013**, *68*, 1−10.
(44) Handke, M.; Handke, B.; Kowalewska, A.; Jastrzębski, W. New Polysilsesquioxane Materials of Ladder-like Structure. *J. Mol. Struct.* **2009**, *924−926*, 254−263.
(45) Tomšič, M.; Cerar, J.; Jamnik, A. Supramolecular Structure vs. Rheological Properties: 1,4-Butanediol at Room and Elevated Temperatures. *J. Colloid Interface Sci.* **2019**, *557*, 328−335.
(46) Zetterström, P.; Dahlborg, U.; Wannberg, A. Structural Studies of Liquid 2-bromopropane and 2-chloropropane by Neutron Diffraction. *Mol. Phys.* **1994**, *83*, 971−981.
(47) Hassion, F. X.; Cole, R. H. Dielectric Properties of Liquid Ethanol and 2-Propanol. *J. Chem. Phys.* **1955**, *23*, 1756.
(48) Hansen, C.; Stickel, F.; Berger, T.; Richert, R.; Fischer, E. W. Dynamics of Glass-forming Liquids. III. Comparing the Dielectric α- and β-relaxation of 1-propanol and o-terphenyl. *J. Chem. Phys.* **1997**, *107*, 1086.
(49) Döß, A.; Paluch, M.; Sillescu, H.; Hinze, G. Dynamics in Supercooled Polyalcohols: Primary and Secondary Relaxation. *J. Chem. Phys.* **2002**, *117*, 6582.
(50) Lunkenheimer, P.; Wehn, R.; Kohler, M.; Loidl, A. Fast Dynamics in Glass-forming Salol Investigated by Dielectric Spectroscopy. *J. Non-Cryst. Solids* **2018**, *492*, 63−67.
(51) Boese, D.; Momper, B.; Meier, G.; Kremer, F.; Hagenah, J.-U.; Fischer, E. W. Molecular Dynamics in Poly(Methylphenylsiloxane) As Studied by Dielectric Relaxation Spectroscopy and Quasielastic Light Scattering. *Macromolecules* **1989**, *22*, 4416−4421.
(52) Ferry, J. D. *Viscoelastic Properties of Polymers*; John Wiley and Sons: 1980.
(53) Larson, R. G. *The Structure and Rheology of Complex Fluids*, Oxford: 1999.
(54) Xing, K.; Tress, M.; Cao, P.; Cheng, S.; Saito, T.; Novikov, V. N.; Sokolov, A. P. Hydrogen-bond Strength Changes Network Dynamics in Associating Telechelic PDMS. *Soft Matter* **2018**, *14*, 1235−1246.
(55) Duarte, D. M.; Tu, W.; Dzienia, A.; Adrjanowicz, K. Study on the effect of side-chain group on the Segmental Dynamics of Selected Methacrylate Polymers at Ambient and High Pressures. *Polymer* **2019**, *183*, 121860.
(56) Gold, B. J.; Hovelmann, C. H.; Luhmann, N.; Szekely, N. K.; Pyckhout-Hintzen, W.; Wischnewski, A.; Richter, D. Importnace of Compact Random Walsks for the Rhelology of Transient Netweorks. *ACS Macro Lett.* **2017**, *6*, 73−77.
(57) Ge, A.; Tress, M.; Xing, K.; Cao, P.-F.; Saito, T.; Sokolov, A. P. Viscoelasticity in Associating Oligomers and Polymers: Experimental Test of the Bond Lifetime Renormalization Model. *Soft Matter* **2020**, *16*, 390.
(58) Pavan, M. S; Sarkar, S.; Row, T. N. G. Exploring the Rare S—H···S Hydrogen Bond using Charge Density Analysis in Isomers of Mercaptobenzoic Acid. *Acta Crystallogr., Sect. B: Struct. Sci., Cryst. Eng. Mater.* **2017**, *73*, 626−633.
(59) Minecka, A.; Kaminska, E.; Heczko, D.; Tarnacka, M.; Grudzka-Flak, I.; Bartoszek, M.; Zięba, A.; Wrzalik, R.; Śmiszek-Lindert, W. E.; Dulski, M.; Kamiński, K.; Paluch, M. Studying Molecular Dynamics of the Slow, Structural and Secondary Relaxation Processes in Series of Substituted Ibuprofens. *J. Chem. Phys.* **2018**, *148*, 224505.
(60) Buchner, R.; Barthel, J.; Stauber, J. The Dielectric Relaxation of Water between 0°C and 35°C. *Chem. Phys. Lett.* **1999**, *306*, 57−63.
(61) Morineau, D.; Alba-Simionesco, C. Hydrogen-bond-induced Clustering in the Fragile Glass-forming Liquid *m*-toluidine: Experiments and Simulations. *J. Chem. Phys.* **1998**, *109*, 8494.
(62) Muller, M.; Kremer, F.; Stadler, R.; Fischer, E. W.; Seidel, U. the Molecular Dynamics of Thermoreversible networks as studied by Broadband Dielectric Spectroscopy. *Colloid Polym. Sci.* **1995**, *273*, 38−46.
(63) Plazek, D. J.; Ngai, K. L. Resolving the Sub-Rouse Modes by Creep Compliance Measurements in Poly(methyl-para-tolyl-siloxane). *Macromolecules* **2020**, *53*, 3940−3945.

https://dx.doi.org/10.1021/acs.macromol.0c01289
Macromolecules 2020, 53, 10225−10233